Numerical Methods in Civil Engineering

Nonlinear modeling of the infill wall based on the brittle cracking model

A. Keyvani Borujeni*, T. Mahdi**

ARTICLE INFO

Article history:
Received:
December 2016.
Revised:
April 2017.
Accepted:
May 2017.

Keywords:
Infill,
Steel moment frame,
Masonry,
Brittle cracking model,
In-plane behaviour

Abstract:

This paper introduces a new numerical method for the analysis of infilled steel frames with hollow clay blocks. This approach is based on the brittle cracking model of ABAQUS. The results of the in-plane calibration analyses obtained with four experimental tests are presented and discussed. The first test was a bare steel frame used as a control specimen. The second was similar to the first one, but with an infill wall in contact with the frame. In the third specimen, the infill wall was completely separated from the frame. The infill wall of the fourth specimen had full contact at the top of the infill wall to the frame and separated from the columns. In the second part of the study, improved versions of the third and fourth specimens have been investigated numerically. Results reveal that the brittle cracking model can be useful in assessing the behavior of masonry infill walls. Furthermore, it can be concluded that the separation of infill walls from the steel frames is quite helpful in reducing the inappropriate effects of infill walls on the overall behavior of buildings.

1. Intruduction

Recent earthquakes showed the significant contribution of masonry infill walls to the structural response of existing buildings.

Lee et al. (2002)[1] showed that the interaction of the steel frame and unreinforced masonry (URM) infill wall is inappropriate due to their varying stiffness, owing to the fact that, the frame stiffness is significantly less when compared to the URM infill wall. Therefore, the URM infill wall takes most of the seismic loads at the beginning of an earthquake.

Murty et al. (2000) [2] conducted a cyclic experimental study on some frames with masonry infill walls. The results demonstrated that the masonry infilled frame has noteworthy stiffness and strength.

To determine the seismic vulnerability of infilled frames, Al-Chaar et al. (2002) [3] carried out several experimental tests. These results showed that the stiffness of the infilled frame is more than the bare frame.

**Corresponding Author: Ph.D. Student, Road, Housing & Urban Development Research Center, Tehran, IRAN, E-mail: A.keyvani@bhrc.ac.ir*
***Author: Assistant Professor, Road, Housing & Urban Development Research Center, Tehran, IRAN*

As discussed before, the conventional masonry infill wall can lead to extensive damage under earthquake loading. The control of the infill wall participation in seismic action using separating gaps between the infill wall and the frame can be considered as a solution to this problem.

The effect of separating gaps between the infill wall and the frame was investigated by Dawe et al. (2001) [4]. It was seen that the gap (20mm) between the top of the wall and the beam reduced the stiffness of the infilled frame. However, according to the study of Dafnis et al. (2000) [5], the aforementioned gap eliminates the "Arching Action", and therefore reduces the out-of-plane resistance of the infill wall.

Two masonry infilled frames were tested under in-plane cyclic loading by Kuang et al. (2014) [6]. These two specimens had different infill wall configurations: (1) an infill wall with full contact (2) an infill wall separated from the columns. It was seen that the infill wall with full contact suffered more damage than the isolated one. In the first specimen, major cracks occurred, whereas the second specimen displayed minor cracks. In comparison with the first specimen, isolating the infill wall from the columns

preserved the integrity of the infill wall and simultaneously improved its seismic performance.

Apart from isolating the infill walls, other structural systems have been introduced. One such a system is the seismic infill wall isolator sub-frame (SIWIS), introduced by Aliaari et al. (2005) [7]. Another system is the seismic infill wall with horizontal sliding joints. In the latter system, several sliding frictional joints have been installed in the masonry infill wall [8].

In this paper, the behaviors of infilled steel frames with separating gaps are investigated. Two types of infill walls are considered as follows:

1) Infill walls with complete decoupling from the frame.

2) Infill walls with full contact at the top of the wall and separated from the columns.

Currently, the two main approaches used to analyze infilled frames are the macro and micro models.

The macro-model approach constitutes an effective method to analyze the global response of masonry structures. In such an approach, masonry is regarded as an equivalent material. A number of such models have been developed by many authors [9]. In the micro-model approach, it is possible to model the mortar, masonry units and their interfaces separately [10]. The micro-model is probably the best tool available to analyze and understand the behavior of masonry, particularly when dealing with its local response. However, it requires an intensive computational effort. To overcome this problem, Tzamtzis et al. (1994) [11] and Sutcliffe et al. (2001) [12] proposed a simplified micro modeling procedure. In this approach, the properties of mortar and the unit-mortar interface are clamped into a common element. Meanwhile, a separated element is used to represent the masonry unit.

2. Constitutive Material Models

In dealing with masonry, ABAQUS provides three different modeling options; the smeared cracking, the brittle cracking and the damaged plasticity models [18]. Each model is designed for a particular usage. The last two models are usually used for masonry units. The damaged plasticity model is by far the most complex concrete model incorporated in ABAQUS that can be used in any loading regime. However, it is not 'user friendly', as it includes multiple parameters and its calibration can be very challenging. In addition, this model does not allow damaged elements to be deleted from the finite element mesh that can lead to numerical instability of the solution algorithms. On the other hand, the brittle cracking model can be used in any loading regime and is 'user friendly' and easy to calibrate. The main disadvantage of this model is the assumption of linear elastic material behavior in compression. As a result, the model can be reliably used only when the masonry is dominated by the tensile brittle failure.

In many previous works, the concrete damaged plasticity model was used to describe the behavior of the masonry units. In such a model, the two variables that account for the different damage states are the tensile and compressive ones. However, since the behavior of the horizontal hollow clay masonry units is dominated by the tensile brittle failure, the brittle cracking model has been found more appropriate for the present paper.

3. Test Set up

3.1 Material characterization

In the test specimens, hollow clay block was used. Also, the 1:4 cement-sand mortars were used to build the masonry infill wall.

3.2 Test setup description

In the test program, four large-scale one-story steel moment-resisting frame specimens were tested in the Structural Department Laboratory of Road, Housing, and Urban Development Research Centre (BHRC), Tehran, Iran [13]. The bounding frame was designed according to the Iranian Code of Practice with medium ductility. All the columns and beams were *IPB180*, as shown in Figure 1. Each specimen was subjected only to in-plane cyclic loads.

The first specimen was a one-story steel moment-resisting frame without infill wall (Specimen F), whereas, the other three specimens had masonry infill walls. Horizontal hollow clay blocks were used in constructing all the infill walls, as follows:

i) A steel frame with infill wall having full contact to the frame (Specimen I).

ii) A steel frame with infill wall separated from the upper beam and columns, as shown in Figure 1 (Specimen N1).

iii) A steel frame with infill wall having full contact at the top of the wall, but separated from columns, as shown in Figure 1 (Specimen N2).

The specification of all tests is shown in Table 1.

Table.1: Specification of experimental specimens

	Height	Span	Thickness	Gap (mm)	
	H (mm)	L (mm)	T (mm)	Beam	Column
F	3000	3000	-	-	-
I	3000	3000	150	0	0
N1	3000	3000	150	15	15
N2	3000	3000	150	0	40

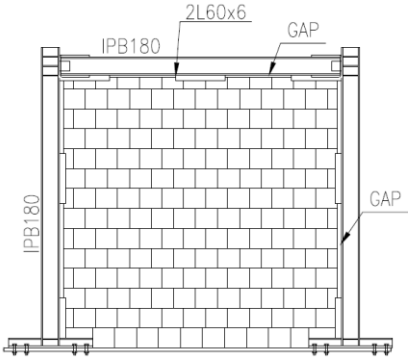

a. (Specimen N1)

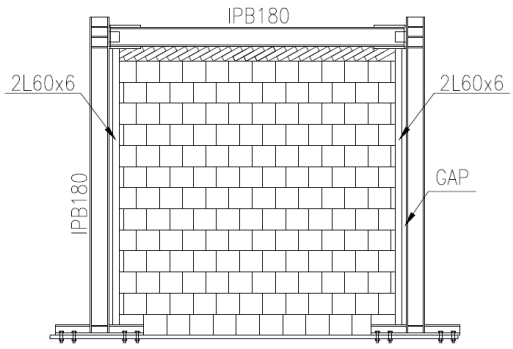

b. (Specimen N2)

Fig.1: The details of experimental specimens

3.3 Loading conditions

To have a general loading history capable of covering the full range of deformation, a new loading protocol was used, as shown in Figure 2. This loading protocol was obtained from combining the ATC-24 [14] and FEMA461 [15] protocols. Both protocols were used in the past to test the seismic performance of structures subjected to cyclic loads. However, the ATC-24 [14] protocol is designed for steel structures, whereas the FEMA461 [15] protocol is found more appropriate for building parts or components sensitive to deformation.

In the third and fourth tests; since gaps between the infill wall and the frame were used, it was assumed that infill walls would not be affected in the early stages of loading. Thus, the ATC-24 [14] protocol was used in these early stages whereas the FEMA461 [15] protocol was used for the other stages.

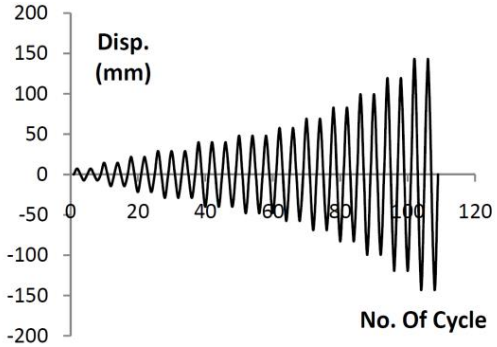

Fig.2: The loading protocol

4. Modeling Concept

4.1 Overall simulation approach

In this paper, the general-purpose nonlinear FE package ABAQUS is used to analyze infilled frames [16]. This model consists of a steel frame connected by contact elements to the masonry infill wall.

4.2 Modeling of the steel frame

The columns and beam have been modeled using the three dimensional solid element (C3D8). The isotropic/kinematic model has been used to model the nonlinear behavior of the steel frame. For more details on the plasticity parameters and their selection, reference is made to Jia et al. (2014) [17]. Table 2 shows the mechanical properties of steel.

Table.2: Mechanical properties of steel material

Equivalent Stress at First Plastic Yield	Hardening Parameter		
	Kinematic		Isotropic
δ_0	C	γ	Q
MPa	MPa	-	MPa
255.9	1617.2	10.7	227.8

4.3 Modeling of the masonry infill wall

The modeling of the masonry has been carried out using the simplified micro-model. According to this model, the properties of the mortar and the unit/mortar interface are lumped into a common interface element, while expanded elements are used to represent the masonry units. These units have been modeled by using the three-dimensional, homogenous solid elements (C3D8).

Generally, it is accepted that a masonry unit exhibits two primary modes of behavior; tensile brittle and compressive ductile ones. Depending on the stress zone (Figure 3), different modes can be chosen for masonry unit modeling. The tensile brittle behavior is represented in the T-T, T-C and C-T zone, where micro cracks merge to form discrete macro cracks with highly localized deformation. The C-C zone represents compressive ductile behavior due to the uniform material degradation where micro cracks develop more or less uniformly throughout the material.

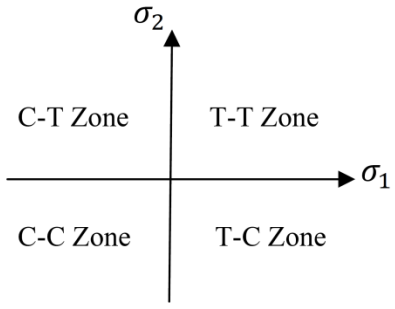

Fig.3: Stress zone

The Rankine criterion has been used to detect the crack initiation. In this criterion, when the maximum principal tensile stress exceeds the tensile strength, cracks are formed. Although the crack detection is based on tension fracture, the cracked behavior includes both tension and shear softening behavior.

The tensile and compressive strength of masonry units have been extensively investigated by many researchers [19], [20] and [21]. Generally, it can be stated that the tensile strength is around 10% of the compressive strength, and it is between 1.5MPa –3.5MPa. The compressive strength of masonry units is around 10MPa –40MPa. Furthermore, based on Moustafa et al. (2012) [22], the elasticity module of the masonry prism is between 1100MPa and 2500MPa.

In this paper, the tensile and compressive strength and the elasticity modulus have been chosen as 1.5MPa, 15MPa and 1500Mpa respectively. The mechanical property of the brittle cracking model is illustrated in Table 3.

The joint between the individual masonry units has been simulated using the interface element (COH3D8). This element empowers the adhesive tensile and shear stresses up to its maximum strength. Since the head joints are not filled with mortar, the load transfer is limited to the bed joints. After surpassing the adhesive stresses in the bed joints, only compressive stresses and frictional forces are transmitted between the single units.

The basic concept of the Coulomb friction model is to relate the maximum allowable frictional stress across an interface to the contact pressure between the contacting bodies. In the basic form of the Coulomb friction model, two contacting surfaces can carry shear stresses up to a certain magnitude across their interface before they slide correspondingly to one another. This state is known as sticking. The Coulomb friction model defines this critical shear stress by the coefficient of friction.

There are two ways to define the basic Coulomb friction model in ABAQUS. In the default model, the friction coefficient is defined as a penalty. Alternatively, the static and kinetic friction coefficients can be identified directly. In this paper, the penalty method has been used and the mechanical properties of the interface elements suggested by Lourenco et al. (1996) [23] have been chosen. These properties are shown in Table 4.

Table.3: Mechanical properties of brittle cracking model

Tensile strength	Shear strength	Elasticity module
f_t	f_c	E
MPa	MPa	MPa
1.5	15	1500

Table.4: Mechanical properties of interface model

Tensile strength	Shear strength
f_t	f_s
MPa	MPa
0.16	0.224
Fraction energy	Fraction energy
G_I	G_{II}
N.mm/mm^2	N.mm/mm^2
0.012	0.05
Tensile stiffness	Shear stiffness
K_t	K_s
N/mm^3	N/mm^3
110	50

4.4 The infill-frame interface

The interface element is capable of simulating both separation and slip. When the surfaces of the frame and infill wall are in contact, it incorporates shear resistance along its interface. There is generally a relationship between this shear resistance and normal stress on the interface. In his paper, the geometrical distance between the column/beam flange and the infill wall has been modeled according to its actual dimension.

5. Numerical Modeling Verification

In this paper, the in-plane behavior has been validated by the experimental results presented by Keyvani and Mahdi (2017) [13].

Figures 4-6 report the lateral load-displacement curves of specimen I, N1, and N2. According to these figures, the load-displacement curves of the present analysis show close agreement to the corresponding experimental ones.

Furthermore, the numerical failure shape of the infill wall is shown in Figures 7c and 9c. These results are in close agreement to those predicted by experimental test, as shown in Figures 7b and 9b.

Thus, it can be concluded that the present numerical analysis can simulate the behavior of the masonry infill wall to an acceptable degree.

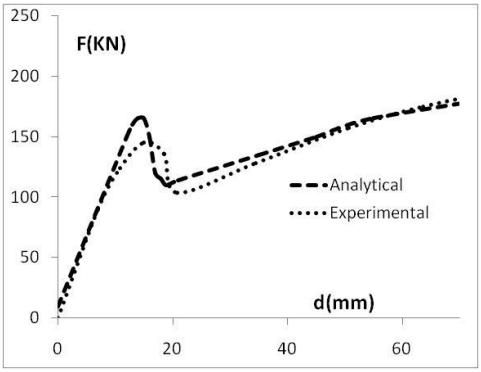

Fig.4: Load-displacement curve (Specimen I)

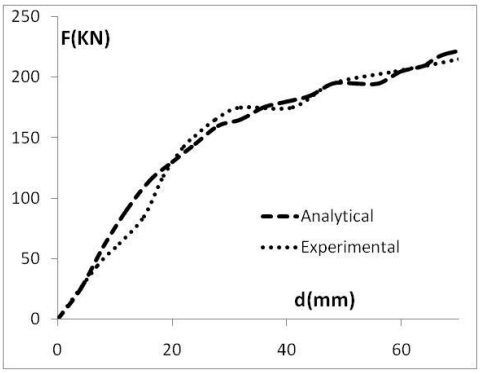

Fig.5: Load-displacement is curve (Specimen N1)

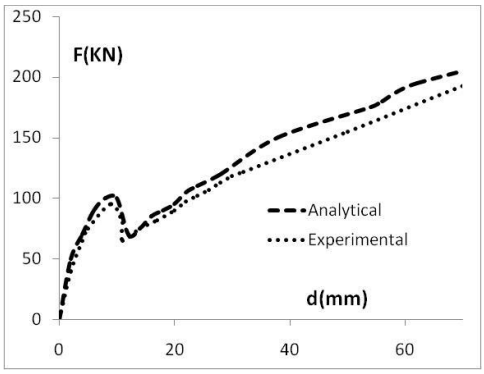

Fig.6: Load-displacement curve (Specimen N2)

a. Experimental

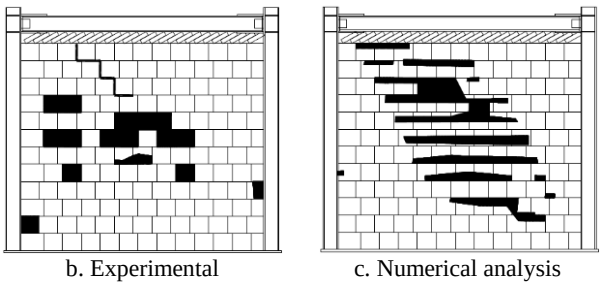

b. Experimental c. Numerical analysis

Fig.7: Failure mode (Specimen I)

a. Experimental

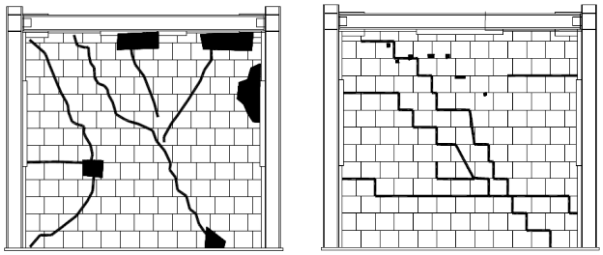

b. Experimental c. Numerical analysis

Fig.8: Failure mode (Specimen N1)

a. Experimental

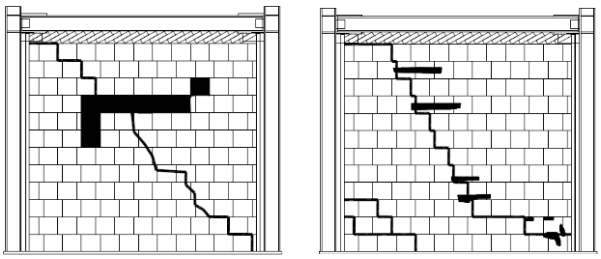

b. Experimental c. Numerical analysis

Fig.9: Failure mode (Specimen N2)

6. Numerical Modeling

As explained before, two arrangements were presented in the test program. The first was an infilled frame with complete separation between the infill wall and the bounding frame. The second was an infilled frame with infill wall having full contact at the top of the infill wall and separated from columns.

In the second arrangement, the infill wall had cracked at low drift. Thus, the performance was not met at the life safety level. This unsuitable behavior was due to the use of unsuitable details. Accordingly, the connection details of the specimens have been changed in the present numerical program. In this respect, six infilled frames have been analyzed by ABAQUS. In each of these cases, the Infilled frame has been subjected to in-plane monotonic loads. The six infilled frames are classified in the following two groups:

Steel frames with infill walls separated from beams and columns, as shown in Figure 10a. The joint cohesive strengths assigned for N1-C1, N1-C2 and N1-C3 are 0.07MPa, 0.1MPa and 0.16MPa respectively.

Steel frames with infill walls having full contact at the top of the infill wall, but separated from columns, as shown in Figure 10b. The joint cohesive strengths assigned for N2-C1, N2-C2 and N2-C3 are 0.07MPa, 0.10MPa and 0.16MPa respectively.

The floor height and bay length were considered equal to those of the calibrated one-bay, one-level laboratory frames, given in Table 1. Table 5 gives the alternative properties of the specimens.

In these specimens, the gap between the top of the infill wall and the beam is based on the recommendation given by Dawe et al. (2001) [4]. Whereas, the gap between the infill wall and two columns is based on the recommendation given by Kuang et al. (2014) [6].

Table.5: Properties of the infilled frames used in the numerical modeling

	Gap(mm)		f_t
Specimen	Beam	Column	MPa
N1-C1	20	20	0.16
N1-C2	20	20	0.10
N1-C3	20	20	0.07
N2-C1	0	40	0.16
N2-C2	0	40	0.10
N2-C3	0	40	0.07

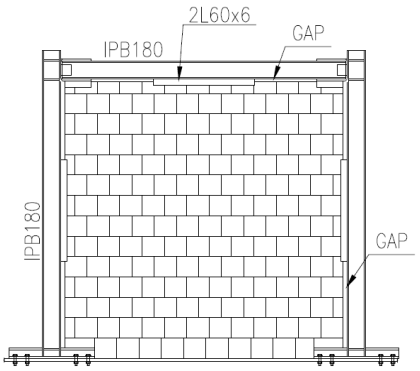

a. (Specimen N1-C1/C2/C3)

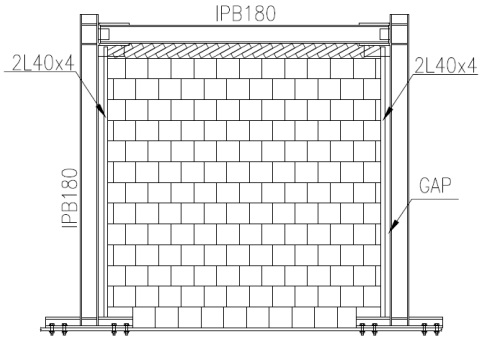

b. (Specimen N2-C1/C2/C3)

Fig.10: The details of numerical specimens

The failure mode and combined stresses/strains of specimens N1-C2 and N2-C2 are plotted in Figures 11 to 16.

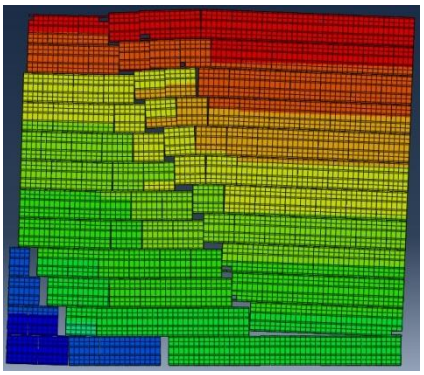

Fig.11: Failure mode of N1-C2

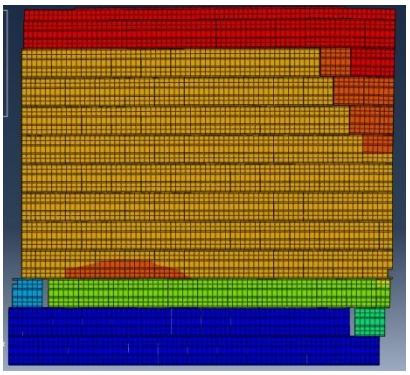

Fig.12: Failure mode of N2-C2

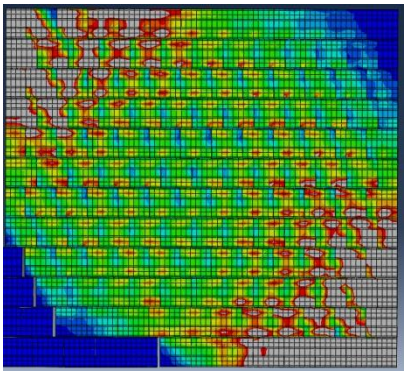

Fig.13: Combined stress of N1-C2

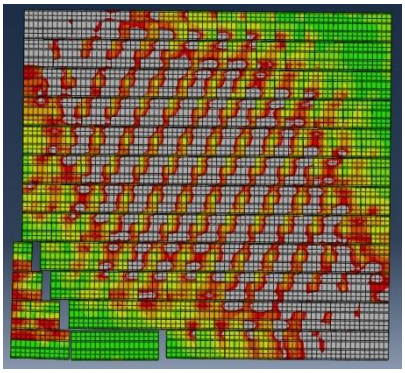

Fig.14: Combined strain of N1-C2

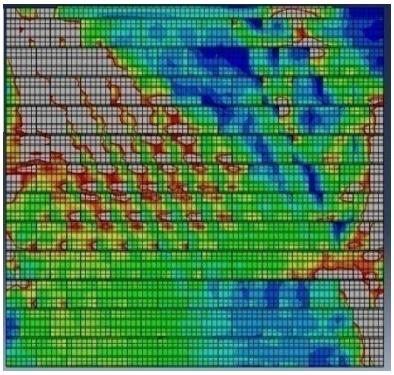

Fig.15: Combined stress of N2-C2

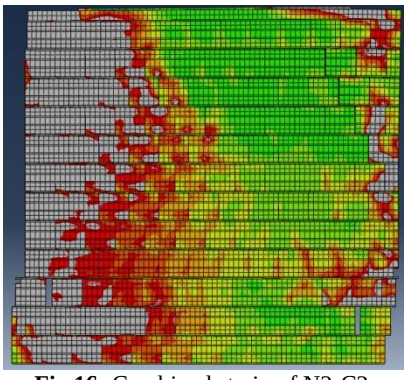

Fig.16: Combined strain of N2-C2

7. Numerical Results

In each of the three specimens N1-C1, N1-C2, and N1-C3, the initial stiffness of the infilled frame is equal to 3200 N/mm. This stiffness is approximately the same as that of the bare frame. The first nonlinearity has been observed at 1.1% drift level combined with some changes in the stiffness. For each of the two specimens N1-C1 and N1-C2, the first crack has occurred in the lower corner of the wall, whereas, for N1-C3, it has commenced in the upper corner of the wall. For these three specimens, the lateral loads at cracking occur at 145, 165 and 165 KN and drift levels occur at 1.1%, 1.7% and 1.7% respectively. Furthermore, the main cracks in these specimens are diagonal ones. These cracks have been developed in the central part of the infill wall and increased gradually in length and width with the increase of the loads. The main cracks have been developed at 2.1% drift for N1-C1 and N1-C2, and 2.6% drift for N1-C3. The specimens achieve their maximum strengths of 220 KN at 3.5% drift level. In N1-C3, due to its low cohesive strength, the cracks have been distributed all over the wall.

In each of the other three specimens, N2-C1, N2-C2, and N2-C3, the initial stiffness of the infilled frame is equal to 3100 N/mm. This stiffness is approximately the same as that of the bare frame. The first nonlinearity has been observed at 1.9% drift level combined with some changes in its stiffness. For each of these specimens, the first crack occurs in the upper corner of the wall. Furthermore, the lateral loads at cracking for N2-C1, N2-C2, and N2-C3 occur at 180, 171 and 163 KN with drift levels at 1.9%, 2.0% and 1.6% respectively. The main cracks in these specimens are horizontal ones and occur at 2.5%, 2.7% and 2.8% drift respectively. The specimens achieve their maximum strengths of 230 KN at the 3.3% drift level.

Based on the present results, it is safe to assume that by using infill walls having separating gaps, trivial effects have been observed on the initial stiffness of the infilled frame. Nevertheless, the stiffness and strength of an infill wall do not play important roles in resisting lateral loads before the formation of the main crack. This conclusion can also be reached from comparing the load-displacement curves, shown in Figure 17 and 18. However, as given in Tables 6-11, all six specimens meet the life safety level for non-structural members.

The results of infilled frames with the different types of frame-infill connection schemes are shown in Figure 19. As shown in this figure, the presence of the infill wall in specimen I causes a significant increase in the overall structural stiffness in the early stages of loadings. Such an increase leads to an increase in the attracted lateral load and may result in rapid failure of the infill wall. On the other hand, the separation between the infill wall and the bounding frame (Specimens N1 and N2) improves the

overall performance of the structure and delays the initiation of the cracks.

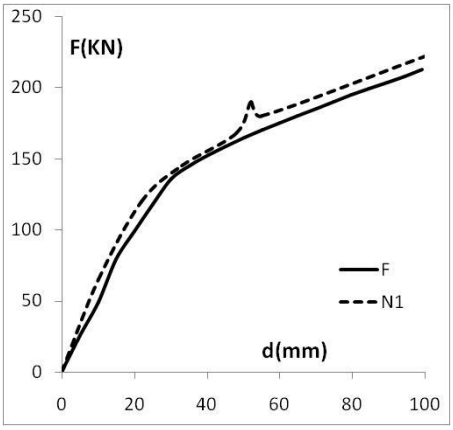

Fig.17: Load-displacement curve of infill wall separated from beam and columns

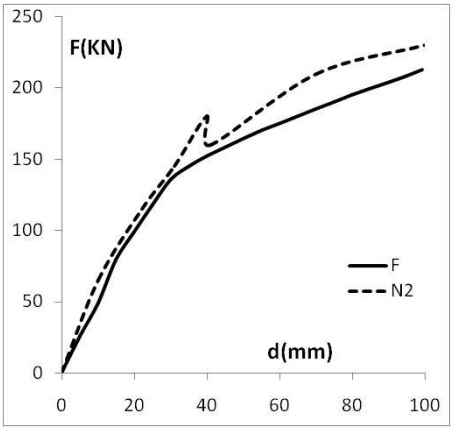

Fig.18: Load-displacement curve of infill wall having full contact at the top, but separated from columns

Table.6: Performance level for Specimen N1-C1

		Drift	Damage
N1-C1	IO	1.1%	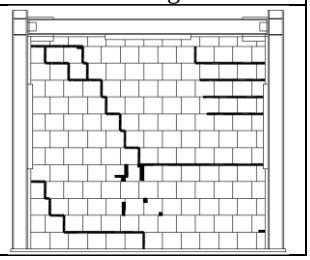
	LS	2.1%	
	CP	3.5%	

Table.7: Performance level for Specimen N1-C2

		Drift	Damage
N1-C2	IO	1.7%	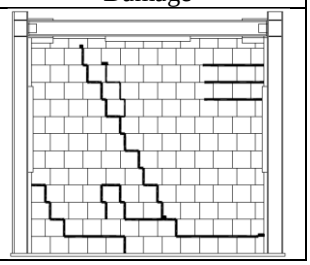
	LS	2.1%	
	CP	3.3%	

Table.8: Performance level for Specimen N1-C3

		Drift	Damage
N1-C3	IO	1.7%	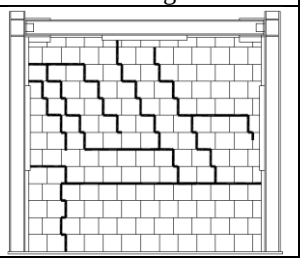
	LS	2.6%	
	CP	3.5%	

Table.9: Performance level for Specimen N2-C1

		Drift	Damage
N2-C1	IO	1.9%	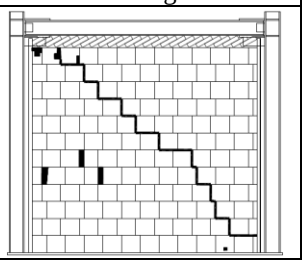
	LS	2.5%	
	CP	3.2%	

Table.10: Performance level for Specimen N2-C2

		Drift	Damage
N2-C2	IO	2.0%	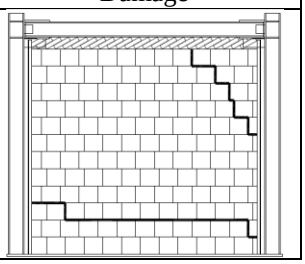
	LS	2.7%	
	CP	3.3%	

Table.11: Performance level for Specimen N2-C3

		Drift	Damage
N2-C3	IO	1.6%	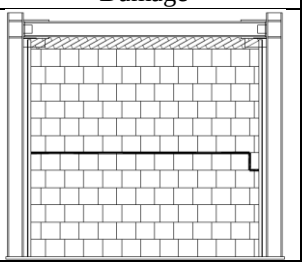
	LS	2.8%	
	CP	3.8%	

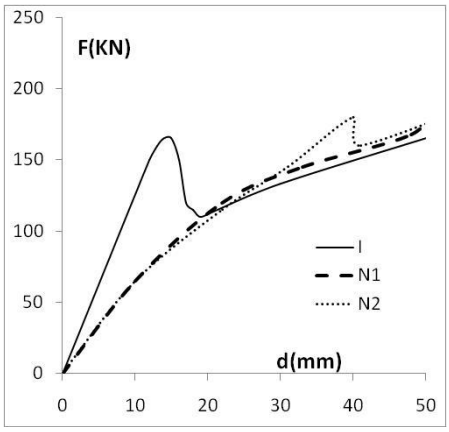

Fig.19: The load-displacement curves (Specimen I, N1-C1 and N2-C1)

8. Conclusions

On the basis of the results presented in this paper, the following conclusions are drawn:

a) The brittle cracking model is suitable for assessing the behavior of masonry infill walls.

b) Full-contact infill walls increase the initial stiffness and attract higher lateral loads that may cause damage at a lower drift level.

c) By separating the infill wall from the frame, the frame-infill interaction is minimized and the damage to the infill wall is reduced, resulting in a better overall behavior of the structure.

References

[1] Lee H.S., Woo S.W. , "Effect of Masonry Infills on Seismic Performance of a 3-Storey R/C Frame with Non-Seismic Detailing", Earthquake Engng Struct. Dyn, 2002, 31:353-378.

[2] Murty C. V. R. and Jain S. K., "Beneficial influence of masonry infill walls on seismic performance of RC frame buildings", Proceedings of 12th WCEE, 2000, pp 1790.

[3] AL-Chaar, G., ISSA, M. and Sweeney S., "Behavior of masonry- infilled no ductile reinforced concrete frames", J. of Struct. Eng., 2002, 128(8), pp. 1055-1063.

[4] Dawe J.L., Y. Liu, and C.K. Seah, "A parametric study of masonry infilled steel Frames", NRC Research Press Web site on February 5, 2001

[5] Dafnis, A., H. Kolsch and H. Reimerdes, "Arching in Masonry Walls Subjected to Earthquake Motions." Journal of Structural Engineering , 2002, 128(2): 153-159.

[6] Kuang J. S. And Wang Z., "Cyclic Load Tests Of RC Frame with Column-Isolated Masonry Infills", Second European Conference on Earthquake Engineering and Seismology, Istanbul, Aug, 2014, 25-29

[7] Aliaari M, and Memari AM, "Analysis of masonry infilled steel frames with seismic isolator subframes", Engineering Structures, 2005, 27(4): 487-500

[8] Preti MM, Bettini NN, Plizzari GG, "Infill walls with sliding joints to limit infill-frame seismic interaction: Large-scale experimental test", Journal of Earthquake Engineering, 2012, 16(1):125-141

[9] Furtado A., Rodrigues H., Arede A., "Modelling of masonry infill walls participation in the seismic behaviour of RC buildings using OpenSees", Int. J. Adv. Struct. Eng., 2015, 7:117–127

[10] Akbarzade, A.A. and Tasnimi A.A., "Nonlinear Analysis and Modeling of Unreinforced Masonry Shear Walls Based", JSEE, winter, 2010, Vol. 11, No. 4

[11] Tzamtzis, A.D., "Dynamic Finite Element Analysis of Complex Discontinuous and Jointed Structural Systems Using Interface Elements", Ph.D. Thesis, Department of Civil Engineering, QMWC, University of London, 1994

[12] Sutcliffe, D.J., Yu, H.S., and Page, A.W., "Lower Bound Limit Analysis of Unreinforced Masonry Walls", Comput. Structure, 2001, 79, 1295- 1312.

[13] Keyvani, A. and Mahdi T., "Reducing the In-plane Effect of Infill on Steel Moment Frame", International Journal of Steel Structures, September 30, 2017

[14] ATC-24, "Guidelines for Cyclic Seismic Testing of Components of Steel Structures for Buildings", Report No. ATC-24, Applied Technology Council, Redwood City, CA. 1992

[15] Federal Emergency Management Agency, "Interim Testing Protocols for Determining the Seismic Performance Characteristics of Structural and Nonstructural Components", FEMA Report 461, Washington, 2007

[16] Simulia, "Abaqus FEA. Providence: Dassault Systèmes Simulia Corporation", 2014

[17] Jia. LJ and Kuwamura H., "Prediction of Cyclic of Mild Steel at Large Plastic Strain Using Coupon Test Results", journal of structural engineering,140(2), 2014

[18] Vilnay M., Chernin L., Cotsovos D., "Advanced Material Modelling of Concrete in Abaqus", 9th International Concrete Conference: Environment, Efficiency and Economic Challenges for Concrete, At University of Dundee Cite this publication, 2014

[19] Crisafulli F. J., "Seismic behaviour of reinforced concrete structure with masonry infill", A thesis for doctor of philosophy, department of civil engineering, university of Canterbury, New Zealand, 1997

[20] Van Der Pluijm, R., "Material properties of masonry and its components under tension and shear", 6th Canadian Masonry Symposium. Saskatchewan Canada, 1992, 675-686

[21] Stavridis, A. & Shing., P.B., "Finite Element Modeling of Nonlinear Behavior of Masonry-Infilled RC Frames", In. Journal of Structural Engineering, 136(3): 285–296

[22] Moustafa A., "Earthquake-Resistant Structures–Design, Assessment and Rehabilitation", Published by InTech Janeza Trdine 9, 51000 Rijeka, Croatia, 2012

[23] Lourenco, P.B., "Computational strategies for masonry structures", PhD diss., TU Delft, Delft University of Technology, 1996